

# Senescent phenotype of astrocytes leads to microglia activation and neuronal death

Wenyou Zhang<sup>1</sup>, Xuehan Yang<sup>1</sup>, Jingyue Liu<sup>1</sup>, Yichen Pan<sup>2</sup>, Ming Zhang<sup>1</sup>, Li Chen<sup>1,3</sup>

<sup>1</sup>Department of Pharmacology, Nanomedicine Engineering Laboratory of Jilin Province, College of Basic Medical Sciences, Jilin University, Changchun, Jilin 130021, China

<sup>2</sup>School of Life Sciences, Jilin University, Changchun, Jilin 130021, China

<sup>3</sup>School of Nursing, Jilin University, Changchun, Jilin 130021, China

**Correspondence to:** Li Chen, Ming Zhang; **email:** [chenl@jlu.edu.cn](mailto:chenl@jlu.edu.cn), [zhangming99@jlu.edu.cn](mailto:zhangming99@jlu.edu.cn)

**Keywords:** aging, microglia activation, senescent phenotype of astrocytes, cell-to-cell interaction, neurons

**Received:** September 8, 2021

**Accepted:** August 11, 2022

**Published:**

**Copyright:** © 2022 Zhang et al. This is an open access article distributed under the terms of the [Creative Commons Attribution License](https://creativecommons.org/licenses/by/3.0/) (CC BY 3.0), which permits unrestricted use, distribution, and reproduction in any medium, provided the original author and source are credited.

## ABSTRACT

**Astrocyte, the most abundant cell type in the central nervous system, is increasingly recognized and is thought to depend on curial and diverse roles in maintaining brain homeostasis, the blood-brain barrier, secrete neurotrophic factors and regulate synaptic transmission which is essential to tune individual-to-network neuronal activity. Senescence in astrocytes has been discovered to be an important contributor to several age-related neurological diseases like Alzheimer's and Parkinson's disease. However, the latest research about astrocytes from aged subjects is not yet adequate to elucidate their crucial process in the regulation of brain function. In this study, aged mice were housed for 4, 18 and 26 months, and cell model of aged astrocytes was constructed by serial passaging until passage 20–25. Meanwhile, oxidative induced astrocytes senescence model was also constructed by H<sub>2</sub>O<sub>2</sub> induction. Our results indicated that in aged mice, the changes in the morphological structure of mitochondria occurs and *in vitro* study indicated that aged astrocytes showed manifest changes in several established markers of cellular senescence like P53, P21, the release of inflammatory cytokine IL-6 and SA-β-gal positive cells. Results also showed mitochondrial dysfunction in the oxidative stress-induced astrocytes senescence model and treatment of berberine could ameliorate these alterations. What's more interests us is that those two types of senescent astrocytes' conditioned medium co-cultured with neuronal cells could do impact on neuron apoptosis no matter in direct or indirect ways. This study may help us better understand the fundamental role of astrocytes senescence on the regulation of normal and pathological brain aging.**

## INTRODUCTION

Aging is a major risk of numerous human diseases. As the elderly population has been expanding rapidly, the growing prevalence of age-related diseases and disabilities is a major public concern. Arguably, one of the most devastating is the changes that occur in the central nervous system, leading to the loss of cognitive, motor, and emotional function that in essence make us who we are. When aging comes, all

those brain cells could be undergoing the process of senescence. Recent studies have demonstrated that clearance of senescent cells results in prolonged life span in mice [1]. Researches [2, 3] published in Nature simultaneously reported that organ aging is an “asynchronous” process, and various types of cells as the basic unit of organ composition also follow this “asynchronous” feature. As is well known, the mammalian brain is composed of a multitude of cell types like astrocytes, microglia, and neurons, so here

leaves the question that is there a precedence among this different type of cells and how they interact and affect each other.

Astrocytes are the predominant glial cells in the brain and serve multiple functions including maintaining the formation of brain, secreting various extracellular matrix proteins and neurotrophic factors, also regulate the transmission efficiency at pre- and post-synaptic sites, and modulate synapse formation and turnover [4]. Thus, astrocytes play crucial roles in maintaining normal brain function and homeostasis [5, 6]. Meanwhile, microglia, the resident macrophages of the central nervous system, have been widely considered as a homogeneous population of cells involved in stable brain patterns. Researchers have found that the activation of microglia will do large effect on cells in brain, the most common behavior of these types of cells is to release a large number of inflammatory factors such as IL-1 $\beta$ , IL-6, TNF- $\alpha$  and finally do impact on other cells in brain. However, whatever the mechanism of astrocytes, microglia, other glia cells or endothelial cells in brain, will eventually lead to the functional loss or death of neuron, and ultimately manifest through a variety of physical behaviors. Questions arise as to how astrocytes, microglia, and neurons cross talk with each other actually.

In the present study, we first investigated whether neuronal damage occurs at the same time as aging and cognitive dysfunction happens at the whole animal level, then we explored primary cultures of rat astrocytes with natural senescence and oxidative stress-induced senescence to detect their interaction with microglia and neurons, and, we found that berberine treatment may be an effectively therapeutic approach to protect the mitochondria of astrocytes from malfunction.

## **MATERIALS AND METHODS**

### **Animals**

Male C57bl6/J mice (8-week-old) were purchased from Vital River Laboratory Animals Technology Co, Ltd [SCXK (Jing) 2016-0006], housed in a temperature and climate condition-controlled barrier system ( $23 \pm 2^\circ\text{C}$  and 45~60% relative humidity, 12 h light-dark cycle) and fed regular rodent chow (Laboratory Animal Center of Jilin University). Animal welfare and experimental procedures complied with the Provisions and General Recommendations of the Chinese Experimental Animals Administration Legislation. All animal experimental procedures were approved by the Ethics Committee for the Use of Experimental Animals of College of Basic Medical

Sciences, Jilin University [SCXK (Jing) 2014-0004]. The animals were acclimated to the laboratory for at least 7 days before use in the experiments. After that, the mice were divided into 3 groups for analysis: 4-month-old mice (young;  $n = 10$ ), 18-month-old mice (initial old group;  $n = 10$ ), 26-month-old mice (aged group;  $n = 10$ ). All animal experimental procedures were approved by the Ethics Committee for the Use of Experimental Animals of College of Basic Medical Sciences, Jilin University [SCXK (Jing) 2014-0004]. Mice were sacrificed under isoflurane inhalation anesthesia until indicated months of age, and then the brains were removed.

### **Tissue processing**

Fresh brain tissues were dissected and soaked overnight in 4% paraformaldehyde, dehydrated in an ascending ethanol series, and equilibrated with xylene, followed by embedding in paraffin and sectioning into 6  $\mu\text{m}$  slices. Then, the samples were dewaxed with xylene and a descending ethanol series.

### **Reagents**

Berberine dilutions were obtained from a 10 mM berberine chloride stock solution prepared in Dimethyl sulfoxide.

### **The Morris water maze (MWM) test includes two main parts**

The place navigation test and the spatial probe test. The study was conducted in a quadrant of a 1.8-m-diameter pool with an 8.5-cm-diameter platform submerged in opaque water. Water remained at temperature ( $22 \pm 1^\circ\text{C}$ ) through all trails. Distinct visual cues were present in all trials. The place navigation test was performed by giving four trials a day with 20- to 30-min intervals between trials for 5 days. The spatial probe test took place 24 hours after the last place navigation test. The spatial probe was performed on the sixth day with the escape platform removed, the probe trials were conducted for 60 s. In the probe trial, the frequency of platform crossings, swimming speed, swimming path length and the time spent in the target quadrant were measured. The training and probe trials were recorded by a video camera mounted on the ceiling, and data were analyzed by using SMART v.3.0.06 (a product of Panlab Harvard Apparatus®).

### **Cell culture and primary astrocytes cultures**

Mouse BV2 and Neuro-2a (N2a) cell lines were purchased from National Collection of Authenticated Cell Cultures (Shanghai, China) and were maintained in

DMEM/F12 supplemented with 10% fetal bovine serum (FBS), 2 mM l-glutamine, 100 IU·ml<sup>-1</sup> penicillin, 100 µg·ml<sup>-1</sup> streptomycin and reseeded at a 1:7 dilution every 3 days. Primary rat astrocytes were isolated from 1- to 2-day-old Wistar rat pups as described previously [7]. In brief, cortices were removed from the rat pups; the meninges were stripped and homogenized. After incubation with trypsin (0.05%) for 30 min in a 37°C thermostatic shaker, the homogenate was resuspended in a trypsin inhibitor/DNase solution, triturated, and dissociated cortical cells were suspended in DMEM/F12 (Life Technology, 11965-084) containing 25 mM glucose, 4 mM glutamine, 1 mM sodium pyruvate, 100 IU·ml<sup>-1</sup> penicillin, 100 µg·ml<sup>-1</sup> streptomycin, and 10% FBS and plated on poly-L-lysine coated 10 cm dishes at a density of  $1 \times 10^5$  cells cm<sup>2</sup> at 37°C with 5% CO<sub>2</sub> in air. 24 hours later, the culture medium was changed to fresh medium. Monolayers of type 1 astrocytes were obtained 7 days after plating. Non-astrocytic cells such as microglia and neurons were detached from the flasks by shaking and removed by changing the medium. Cells were trypsinised and reseeded at a 1:3 dilution every 3 days on poly-L-lysine coated 10 cm dishes.

### Senescence induction

Induction of astrocytes senescence by oxidative stress was performed as previously described [8]. In brief, early-passage (no more than five passages) astrocytes were incubated for 24 h, then the medium was removed and 80 µM H<sub>2</sub>O<sub>2</sub> in complete astrocyte culture medium was added for 2 h, then the medium was removed and washed with PBS, after that, cells were cultured in medium without serum for 24 hours. Induction of astrocyte senescence by natural senescence was performed by trypsinizing astrocytes when reaching 80–90% confluency, primary rat astrocytes isolated from 1- to 2-day-old Wistar rat pups were defined as passage 0, the number of passages increases when the cells trypsinized for on time. Cells within passage 20–25 were used as aged-astrocytes and within passage 1–5 were used as young-astrocytes.

### Senescence-associated-β-galactosidase (SA-β-gal) staining

β-galactosidase activity was measured using the Senescence β-Galactosidase Staining Kit (Beyotime, Shanghai, China). Briefly, cells were washed with PBS and fixed with 1× fixative solution for 15 min. Then, β-galactosidase staining solution with a final pH between 5.9 and 6.1 was prepared and added to the fixed cells. Samples were sealed with parafilm to prevent evaporation and placed in 37°C incubator without CO<sub>2</sub> overnight. Imaging was performed using an inverted microscope.

### Preparation of astrocytes-conditioned medium and microglia-conditioned medium

Astrocytes were grown in 96-well plates, when reaching 80% confluency, cells were treated with 80 µM H<sub>2</sub>O<sub>2</sub> or normal culture medium for 2 h, then the medium was removed and washed with PBS for 1 time and DMEM/F12 without serum was added for 24 h, finally the supernatant was collected for downstream experiments. Conditioned medium from microglia was collected after treating with astrocytes conditioned medium for 24 h.

### MTT assay

Cell viability was determined using a modified MTT assay [9]. Briefly, 5000 cells well<sup>-1</sup> were plated in 96-well plates and incubated overnight. Cells were then treated with conditioned medium for 24 h. At the end of the follow-up period, MTT in PBS was added and the cultures were incubated for 2 h at 37°C incubator. After discarding the supernatant, the formazan was dissolved in DMSO; then, the optical density (OD) values were determined at 492 nm. The cell viability was calculated by taking the cell viability in the non-treatment group as 100%.

### ATP measurement

Intracellular ATP level was determined by ATP assay kit (Beyotime, Shanghai, China), which can perform cell lysis and generate a luminescent signal proportional to the amount of ATP present. The preparation of samples was conducted according to the manual of the product. The supernatants of each sample (20 µL) were added to the ATP detection solution (100 µL) attached to the kit. Then, Infinite 200 Pro (Tecan) was utilized to record the RLU values. The protraction of the standard curve was conducted on the basis of the RLU values of ATP with the concentration of 0, 0.01, 0.05, 0.1, 0.5, 1, 5, and 10 nmol/L. Finally, the protein concentration was used to standardize the results, which were presented as ATP/protein (nmol/mg).

### Mitochondrial membrane potential

Mitochondrial membrane potential ( $\Delta\Psi_m$ ) loss was assessed by a Mitochondrial Membrane Potential Assay Kit with JC-1. After treatment for 24 h, cells were incubated with JC-1 for 20 min, washed and visualized under BX53 fluorescence microscope (Olympus). Red fluorescence indicates normal  $\Delta\Psi_m$  with JC-1 aggregates in mitochondria, and green reflects cytosolic JC-1 monomer indicating  $\Delta\Psi_m$  loss.

## Western blot analysis

The harvested cells were digested by RIPA buffer, following sonication, the samples were centrifuged for 15 min at 12,000 g at 4°C. For the determination of total protein density, a BCA Protein Assay Kit (Thermo Fisher) was applied. Then, after separating the proteins on SDS-PAGE, the proteins were transferred onto the PVDF membrane (Millipore). In all, 5% non-fat milk was utilized for the sealing of membranes in Tris-buffered saline (pH 7.5). The membrane went through overnight hybridization with the primary antibodies and second antibodies. The protein bands were revealed by an ECL kit (Thermo Fisher). The expression levels of proteins were evaluated by Image J (National Institutes of Health, USA). The primary antibodies were: anti-P53 (Proteintech), anti-P21 (Proteintech), anti-P16 (Abcam), anti-OPA-1 (Proteintech), anti-Mfn2 (Abcam), anti-DRP-1 (Proteintech), anti- $\beta$ -actin (Proteintech).

## HE staining

Fixed, paraffin-embedded brain tissue was sectioned and underwent hematoxylin eosin (HE) staining according to the following procedure. Sections were deparaffinized, washed in distilled water, and incubated in hematoxylin solution for 5 min; excess hematoxylin solution was washed off with running tap water. To remove background staining, sections underwent a differentiation step in hydrochloric acid alcohol with fully washed in running tap water. Sections were then counterstained in eosin solution for 2–3 min, washed in running tap water, dehydrated through graded alcohol, and mounted with neutral resin. Pathological changes in neurons were observed under a light microscope CX31 (Olympus).

## Nissl staining

Paraffin-embedded, fixed brain tissue was deparaffinized, washed 1–2 min in distilled water, dipped in 1% thionin lysol at 37°C for 30 min, and washed again for 1–2 min in distilled water. To moderately differentiate the nucleus, sections were incubated in 0.5% hydrochloric acid alcohol, washed back to blue, and differentiated using 95% alcohol until the Nissl substance was visualized. Sections were then dehydrated (twice for 5 min each) in 100% anhydrous alcohol, permeabilized with xylene twice (5 min each), and mounted with neutral gum. Changes observed in neurons and Nissl bodies of the hippocampal CA1, CA2, CA3 and DG regions were detected under a light microscope CX31 (Olympus).

## Immunofluorescence and immunohistochemistry

Total cells on the slides went through permeabilization in 0.3% Triton X-100 subsequent to the fixation in 4%

paraformaldehyde. After that, goat serum was utilized for blocking. Cells or tissues were later cultivated overnight with anti-GFAP (Abcam). Then, the slide was subjected to 1-h incubation with the Fluorescein (PE)-conjugated Affinipure Goat Anti-Mouse IgG (H+L) (Proteintech) under the room temperature, again, cells or tissues were cultivated overnight with anti-beta-Galactosidase (Proteintech) or P16<sup>INK4a</sup> (Proteintech) at 4°C and then subjected to 1 h incubation with the FITC-conjugated Goat Anti-Rabbit IgG(H+L) (Proteintech). The counterstaining of the nucleus was accomplished by using DAPI. For immunohistochemistry (IHC), slides were incubated in 0.9% H<sub>2</sub>O<sub>2</sub> for 30 min. Afterwards, the slides were placed in blocking buffer (goat serum 1:20 in PBST/BSA) for 30 min at room temperature. And then anti-Iba1 (Abcam) antibody was used, tissues were further blocked with Biotin for 10 min each. Antibodies were detected using a rabbit peroxidase ABC Kit (MXB biotechnologies). Each sample was viewed with BX53 Fluorescence microscope (Olympus).

## Iba1+ cell density and soma size quantifications

Scans of the hippocampus were imaged using BX53 Fluorescence microscope (Olympus) in bright field on IHC sections stained for Iba1. The number of Iba1+ cells and the area were recorded. Cell numbers were expressed as number of Iba1+ cells per mm [10] in a 6  $\mu$ m thick section. The area of the soma of Iba1+ cells was manually traced and measured in ImageJ.

## Elisa assays

Rat IL-6 Elisa kit (Dakewe Biotech, Thermo Fisher), Mouse IL-1 beta Elisa kit (Dakewe Biotech), Rat IL-1 beta Elisa kit (Proteintech), Mouse IL-6 Elisa kit (Proteintech). Young/aged astrocytes were plated on 12-well plates, after reaching confluency, the medium was removed and DMEM/F12 without serum was added for 24 h, Rat IL-6 and IL-1 beta were detected by collecting the supernatant. Similarly, after culturing with H<sub>2</sub>O<sub>2</sub> treated astrocytes conditioned medium for 24 h, the supernatant of BV2 was collected for detecting Mouse IL-6 and Mouse IL-1 beta.

## Caspase-3 activity determination

Caspase 3 Activity Assay Kit and GreenNuc™ Caspase-3 Assay Kit for Live Cells was purchased from Beyotime (Nanjing, China) was used to calculate caspase-3 activity in cells according to the manufacturer's introductions.

## Electron microscopy

Fresh Hippocampus tissue was cut into 1 × 1 × 2 mm<sup>3</sup> samples, fixed in 2.5% glutaraldehyde solution,



embedded, and sliced into ultrathin sections. The ultrastructural changes were observed under a HT-7800 transmission electron microscope (Hitachi).

### Statistical analysis

Data computation was accomplished by SPSS software 16.0 (SPSS Inc., Chicago, IL, USA). For determining the significance of differences between two groups or among multiple groups, Student's *t*-test or one-way ANOVA was applied. Each experiment was conducted for three times at minimum. The statistical significance in differences was confirmed when  $p < 0.05$ .

### Data availability

All the data used to support the findings of this study are included within the article. Additional data related to this paper may be requested from the authors.

## RESULTS

### Cognitive impairment and neuron loss occurred in aged mice

Morris water maze test is a major behavioral testing method for measuring cognitive impairment of rodents. To further explore whether the changes in cognitive function associated with age, 4-, 18-, 26-month-old male mice were chosen as our research subjects. The training phase lasted for 5 days and the mice were placed in a dark circular pool and were allowed to find the hidden platform with 60 s, with four training trails per day. The probe test was performed on the sixth day. As the training progressed, the latency to reach the platform was significantly decreased in the 26-month-old group at the fourth and fifth day (Figure 1A), indicating that the older mice showed significant learning deficiency during the sessions. On the sixth day, the escape platform was removed and the frequency through platform was recorded for a total duration on 60 s. Three typical movement trajectory are presented (Figure 1B), the time and path length in the target quadrant, the swimming speed, the tracking pathway and the latency to location were also analyzed (Figure 1C–1G). The 4-month-old mice spent the least amount of time to get the location of the original platform and took much more times swimming through the platform (Figure 1C, 1D). Compared with the 4-month-old mice, the 18-month-old mice and 26-month-old mice spent much more time and used a longer path to reach the platform (Figure 1F, 1G). In addition, the average speed was lower in the 18-month-old mice and the 26-month-old mice than in the 4-month-old mice (Figure 1E), but without significantly different from each

other. Since the data show differences in behavioral test, and the hippocampus is a crucial structure in memory circuits and is firstly and foremostly responsible for memory and learning functions, the HE [11] and Nissl staining were made to see whether the structural integrity of the hippocampus was changed or the neurons start to lose. HE staining of the hippocampal neurons revealed normal neurons in the group of 4-month-old mice with rich cytoplasm and slightly and round stained nucleus and clear formation, on the contrary, in the group of 24-month-old mice, degenerated neurons showed shrinking cytoplasm and bodies, and most of the degenerated neurons revealed deep stained nucleus and irregular morphology (Figure 1H). The neuronal loss was evaluated with age. As shown in Figure 1I, 4-month-old mice showed highly dense pyramidal layer neurons with intact structure, in contrast, the neurons appeared atrophied and pyknotic in 26-month-old mice, meanwhile, the numbers were also lower than those in 4-month-old mice, especially in the region of CA1, CA3 and DG, which can be seen intuitively from Figure 1J. In summary, the cognitive impairment and morphological changes may begin to appear in the 18-month-old mice and with age growing, the 26-month-old mice presented more obvious differences from other groups.

### The emergence of senescent astrocytes and activated microglia

A variety of cells exist in the brain, mainly including neurons, astrocytes, microglia, and oligodendrocytes, which type of cells play a key role in the initiation of aging still remains unclear. As is known to all that the expression of  $\beta$ -gal and P16<sup>INK4a</sup> can be used as senescent markers [12]. Here, the 4-month-old mice were defined as young group and the 26-month-old mice were defined as aged group. With the increasing age of mice, the expressions of  $\beta$ -gal and P16<sup>INK4a</sup> was significantly increased (Figure 2A–2D) and most of the positive expression of  $\beta$ -gal and P16<sup>INK4a</sup> were co-stained with GFAP, these phenomena suggest that the senescence of astrocyte may play a role in neuronal degeneration of aging. So, whether changes in the organelle structure of astrocytes occur during the senescent progress, electron microscopy was used to examine the ultra-structure of the mitochondria in astrocytes. The data show that the mitochondria changed from a strip shape to a rounded one with age and the cristae were vague and some of them disappeared (Figure 2E) in aged mice. Meantime, data also indicated that a progressive enlargement of microglial size as the activation state and phagocytic capacity of the cells enhances (Figure 2F–2H), usually, amoeboid microglia was considered as higher activation state [13].

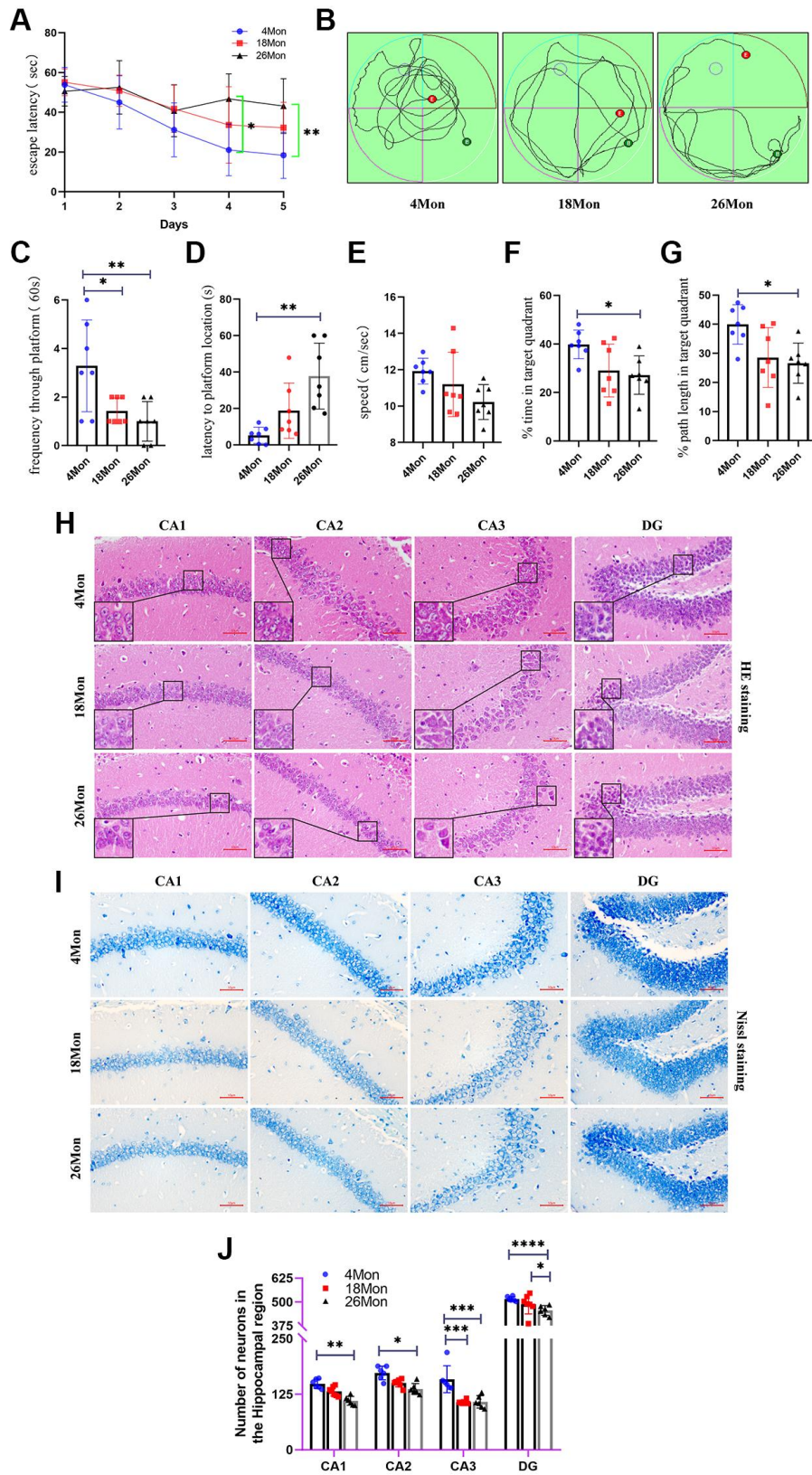


**Figure 1. Age related cognitive impairment and neuron loss in mice.** (A) Escape latency. (B) Movement Trajectory of mice. (C) Frequency through platform. (D) Latency to platform location. (E) The average swimming speed. (F) The percentage of time in target quadrant. (G) The percentage of path length in target quadrant. (H) HE staining of mouse brain. Scale bar, 50  $\mu$ m. (I) Nissl staining in the hippocampus of each group. Scale bar, 50  $\mu$ m. (J) The number of living neurons of hippocampus in mice. All experiments were expressed as the mean  $\pm$  S.D, analyzed by ANOVA followed by Tukey's test, \* $P < 0.05$ , \*\* $P < 0.01$ , \*\*\* $P < 0.001$ , \*\*\*\* $P < 0.0001$ .

## Serial passaged astrocytes show phenotypes of aged cells and affected neuronal viability

To deeply investigate the changes in a range of physiological functions of astrocytes during senescence *in vitro*, astrocytes were isolated from Wistar rat pups and made identification by the marker of GFAP (Figure 3A), the data showed highly purity of astrocytes. To simulate natural senescence, serial passaging under standard culture conditions (passages between 20–25, named as aged-astrocytes) was made and found that SA- $\beta$ -gal positive astrocytes were increased compared with those from passages 1–5, which were named as young-astrocytes (Figure 3A). To systematically explore the altered phenotype of young and aged astrocytes, senescence markers of P53, P16, P21 were tested, and, IL-6, which was collectively known as the senescence-associated secretory phenotype (SASP) [14]

were also performed. As is shown in Figure 3B, 3C, after serial passaging of astrocytes, the expression of P53, P21 and P16 was gradually increased, meanwhile, the concentration of IL-6 in supernatant of aged-astrocytes was elevated either (Figure 3D). Mitochondrial membrane potential was selected to detect whether the mitochondrial function remained normally, notably, the MMP showed significantly decreased in those aged astrocytes (Figure 3E). To confirm whether these changes of astrocytes would do deleterious effects on microglia or neurons, we then examined the neurotoxicity to Neuro-2a cells by treating with young-astrocytes or aged-astrocytes supernatant for 24 h (Figure 3F) As might be expected, aged-astrocytes-derived CM or BV2 supernatant which were treated with those aged-astrocytes-derived CM significantly decreased Neuro-2a cell's viability (Figure 3G, 3J), Meanwhile, aged-astrocytes-derived

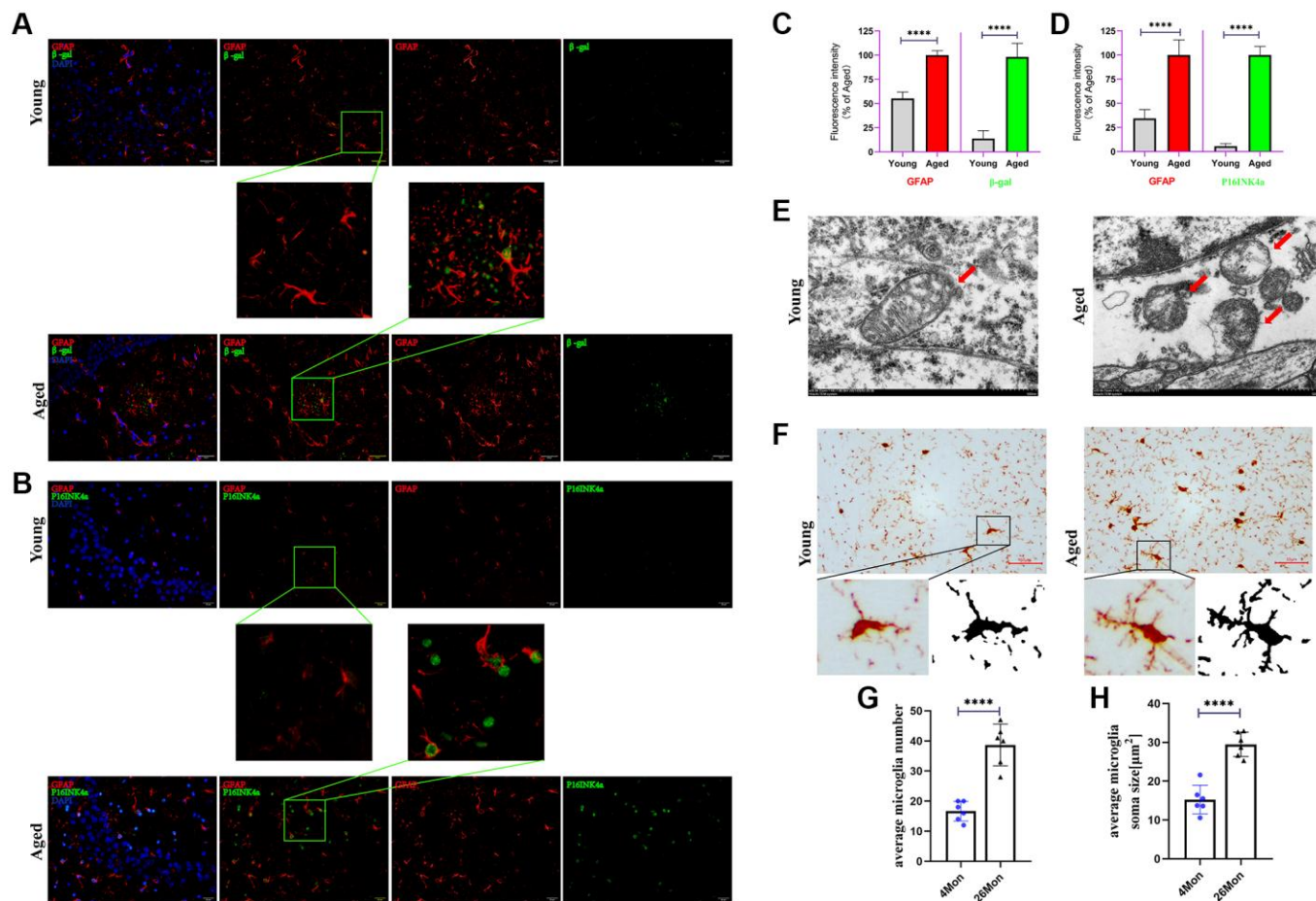


**Figure 2. Senescent astrocytes occurred and accompanied with microglia activation.** (A) Representative brain sections co-immunostained for GFAP (red) and  $\beta$ -gal (green) in young and aged mice (hippocampus).  $\times 200$  magnification. (B) Representative brain sections co-immunostained for GFAP (red) and P16<sup>INK4a</sup> (green) in young and aged mice (hippocampus).  $\times 200$  magnification. (C, D) Quantification of data from (A) and (B) ( $n = 6$  mice/group). (E) Representative transmission electron microphotographs showing mitochondria in astrocytes from hippocampus of young and aged mice. Scale bar, 500 nm. (F) Brain sections immunostained for iba1 (activated markers of microglia). Scale bar, 50  $\mu$ m. (G, H) Quantification of the average soma size and numbers of microglia in the CA3 hippocampal region. All experiments were expressed as the mean  $\pm$  S.D, analyzed by ANOVA followed by Tukey's test, \* $P < 0.05$ , \*\* $P < 0.01$ , \*\*\* $P < 0.001$ , \*\*\*\* $P < 0.0001$ .



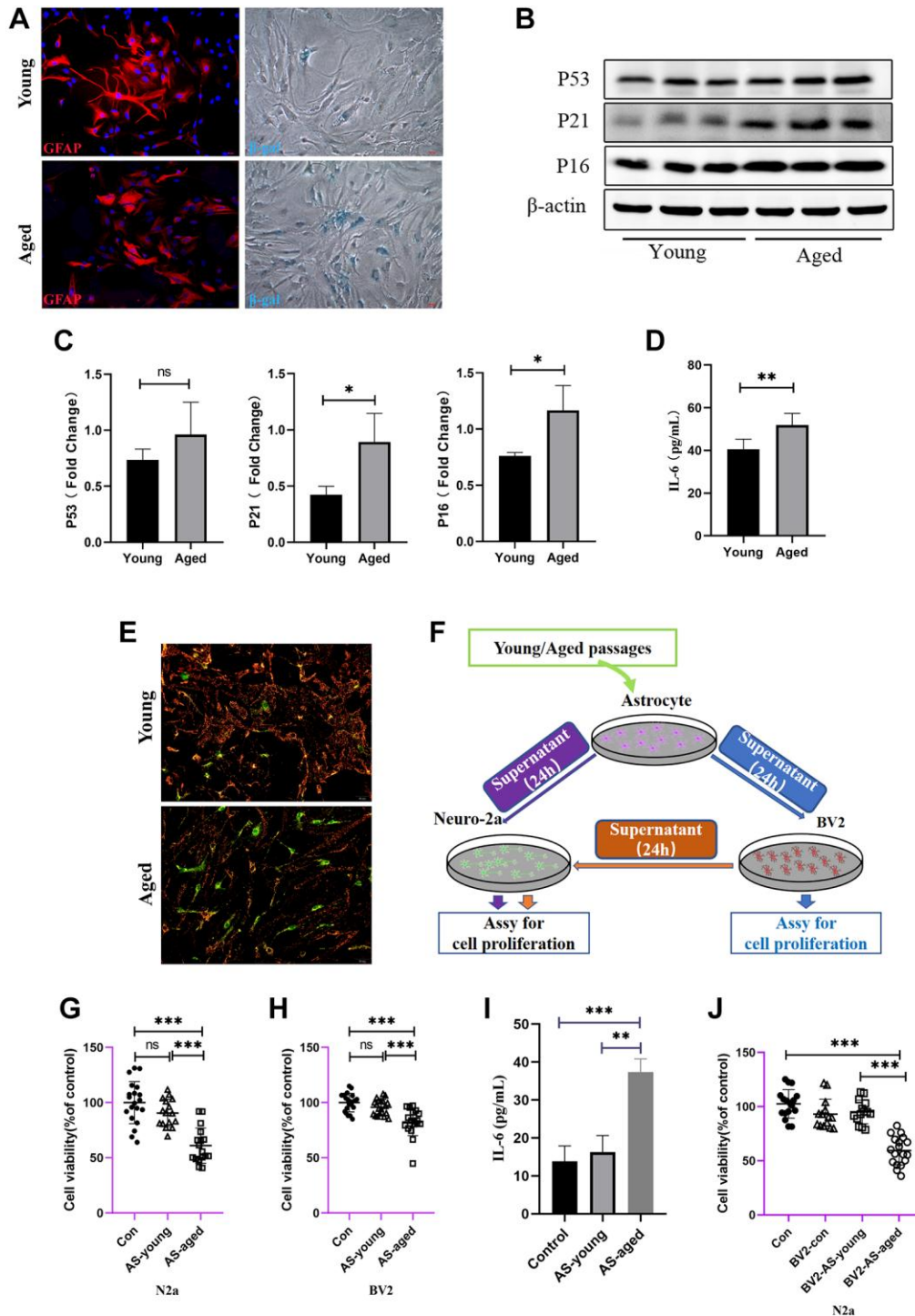


**Figure 3. Astrocytes acquired senescent phenotype through serial passaging and SASP secretion may cause direct or indirect neuronal damage.** (A) Immunofluorescent staining using GFAP antibody as astrocytes' marker, and cell senescence staining of  $\beta$ -gal. (B) Representative immunoblot and (C) Quantitation of P53, P21, P16 and  $\beta$ -actin, in young and aged astrocytes.  $\beta$ -actin was a loading control and data are expressed relative to Young,  $n = 3$ . (D) Cytokine ELISA of IL-6 in culture medium released from Young and Aged astrocyte. (E) JC-1 staining. The red and green fluorescence reflects changes in the mitochondrial membrane potential of young and aged astrocytes,  $n = 3$ . (F) Scheme of conditioned media (CM) and cell viability assay by using young and aged astrocytes or astrocytes-CM treated BV2 cells. (G) Cell viability assay of N2a cells by treating with young and aged astrocytes' supernatant. (H) Cell viability assay of BV2 cells by treating with young and aged astrocytes' supernatant. (I) Cytokine ELISA of IL-6 in culture medium of BV2 treated with young/aged-astrocytes' supernatant. (J) Cell viability assay of N2a cells by treating with supernatant of BV2 cells (treated with supernatant of young and aged astrocytes). All experiments were expressed as the mean  $\pm$  S.D, analyzed by ANOVA followed by Tukey's test, \* $P < 0.05$ , \*\* $P < 0.01$ , \*\*\* $P < 0.001$ , ns represents no significance.



CM promoted negative contribution for the survival of BV2 cells (Figure 3H), at the meantime, the level of IL-6 in BV2 supernatant was increased (Figure 3I), suggests that substances released from aged-astrocytes may cause damage along with activating the BV2 cells and prompt cells to release inflammatory mediators to damage neurons. So, in general, mitochondrial dysfunction may occurred when aging happens, and, in this way, astrocytes can be reactive during aging and release substances that activate nearby astrocytes, microglia and neurons.

### **Astrocytes activate a senescence program in response to oxidative stress and showed mitochondrial dysfunction**

The above experiments were to Mimic natural aging, or in other words, chronic aging of cells during *in vivo* process. Here, another *in vitro* mitochondrion damaged model was established. What is known to all is that throughout the human life cycle, oxidative stress occasionally occurs in the brain or in other organ, and mitochondria are much susceptible to it. In this model, rodent astrocytes were treated with 80  $\mu\text{M}$   $\text{H}_2\text{O}_2$  for 2 h and then removed and added new culture medium without serum for 24 h. This test aim to find the appropriate concentration that would do damage to the mitochondria without affecting the viability at the same time. The cell viability showed no significance when the concentration reached 80  $\mu\text{M}$  (Figure 4A). Next, senescence markers were also detected to find out if the cells already reached the SASP phenotype. As the data shown in Figure 4B, 4C, the proteins expression of P53, P21 and P16 were significantly elevated after treating with  $\text{H}_2\text{O}_2$ . Meanwhile, administration of berberine showed a certain degree of decrease in these indicators, although the expression of P16 decreased but showed no significance. And the concentration of IL-6 in supernatant of astrocytes treated with  $\text{H}_2\text{O}_2$  were elevated compared with those that didn't (Figure 4D). Mitochondrial membrane potential also showed that exogenous  $\text{H}_2\text{O}_2$  treatment caused MMP decrease and administration of berberine would do recovery of the damaged MMP (Figure 4E). ATP production is the most common product produced by mitochondria, compared with control cells,  $\text{H}_2\text{O}_2$  treatment markedly lowered cellular ATP levels (Figure 4F). What is more,  $\text{H}_2\text{O}_2$  treatment might have effect on mitochondrial fission by elevating the expression of mitochondrial fission protein drp1, and decreasing the expression of mitochondrial fusion proteins Mfn2 and opa-1, although the mitochondrial fusion protein showed no significant decrease. Concurrently, the adverse effect caused by  $\text{H}_2\text{O}_2$  on mitochondrial function may play a role in the development of aging; what is more, treatment of berberine seems to have good effect on ameliorating the

mitochondrial function since berberine was usually used as a positive drug against mitochondrial dysfunction (Figure 4G, 4H).

### **Direct interactions between senescent astrocytes and neurons**

To confirm that mitochondrial dysfunction of  $\text{H}_2\text{O}_2$ -treated astrocytes is responsible for neuron viability, the neurotoxicity of Neuro-2a cells by culturing with conditioned medium isolated from  $\text{H}_2\text{O}_2$ -stimulated astrocytes (Figure 5A) was examined. As expected,  $\text{H}_2\text{O}_2$ -treated astrocytes-derived CM significantly decreased the viability of Neuro-2a cells (Figure 5B), however, CM from astrocytes treated without  $\text{H}_2\text{O}_2$  didn't affect the viability of Neuro-2a cells. To confirm if apoptosis happens after treating with conditioned medium for 24 h, we also detected caspase-3 activity of Neuro-2a cells and found that Neuro-2a cells treated with  $\text{H}_2\text{O}_2$ -treated astrocytes supernatant presented a significant increase of caspase-3 activity at 24 h (Figure 5C), what's more, this effect was ameliorated by administration of berberine.

### **Indirect effects of senescent astrocytes to neurons**

As we have shown previously, we found that the conditioned medium of astrocytes treated with  $\text{H}_2\text{O}_2$  could provide direct toxic effects on Neuro-2a cells. However, as we know, the astrocytes may provide some indirect effects on numerous types of cells in the brain by activating microglia cells, which act as immune cells in the brain, making them to secrete neuronal inflammation cytokines thus do the harm to neuronal cells. To confirm this hypothesis and refer to the hypothetical diagram (Figure 6A), we first examined the viability of BV2 cells treated with  $\text{H}_2\text{O}_2$ -stimulated astrocytes or supernatant and found that after culturing with condition medium for 24 h, the viability of BV2 cells was significantly decreased (Figure 6B), what's more interesting is that the IL-6, also seemed as a neuronal toxic cytokine, or SASP, was significantly elevated compared to those treated without  $\text{H}_2\text{O}_2$  (Figure 6C). After treating with  $\text{H}_2\text{O}_2$ -treated astrocytes-derived CM for 24 h, the supernatant of BV2 cells was collected and cultured with Neuro-2a cells. Data showed that after incubation with the conditioned medium of BV2 cells, the viability of Neuro-2a cells decreased significantly compared to other groups (Figure 6D), moreover, the activity of caspase-3 of these Neuro-2a cells showed that the supernatant of BV2 cells (treated with supernatant of astrocyte with or without  $\text{H}_2\text{O}_2$  for 24 h) was also capable of increasing caspase-3 activity of Neuro-2a cells, and administration of berberine would have ameliorating effects (Figure 6E).

## DISCUSSION

Astrocytes play crucial physical and molecular roles in the mammalian brain, any interference to their normal physiological function may lead to the pathology of

central nervous system diseases, thence, the aging of astrocytes may have immense impact on the function and micro-environment of the brain. As a potential candidate of aging, cellular senescence was thought to be the inducing factor of aged-related

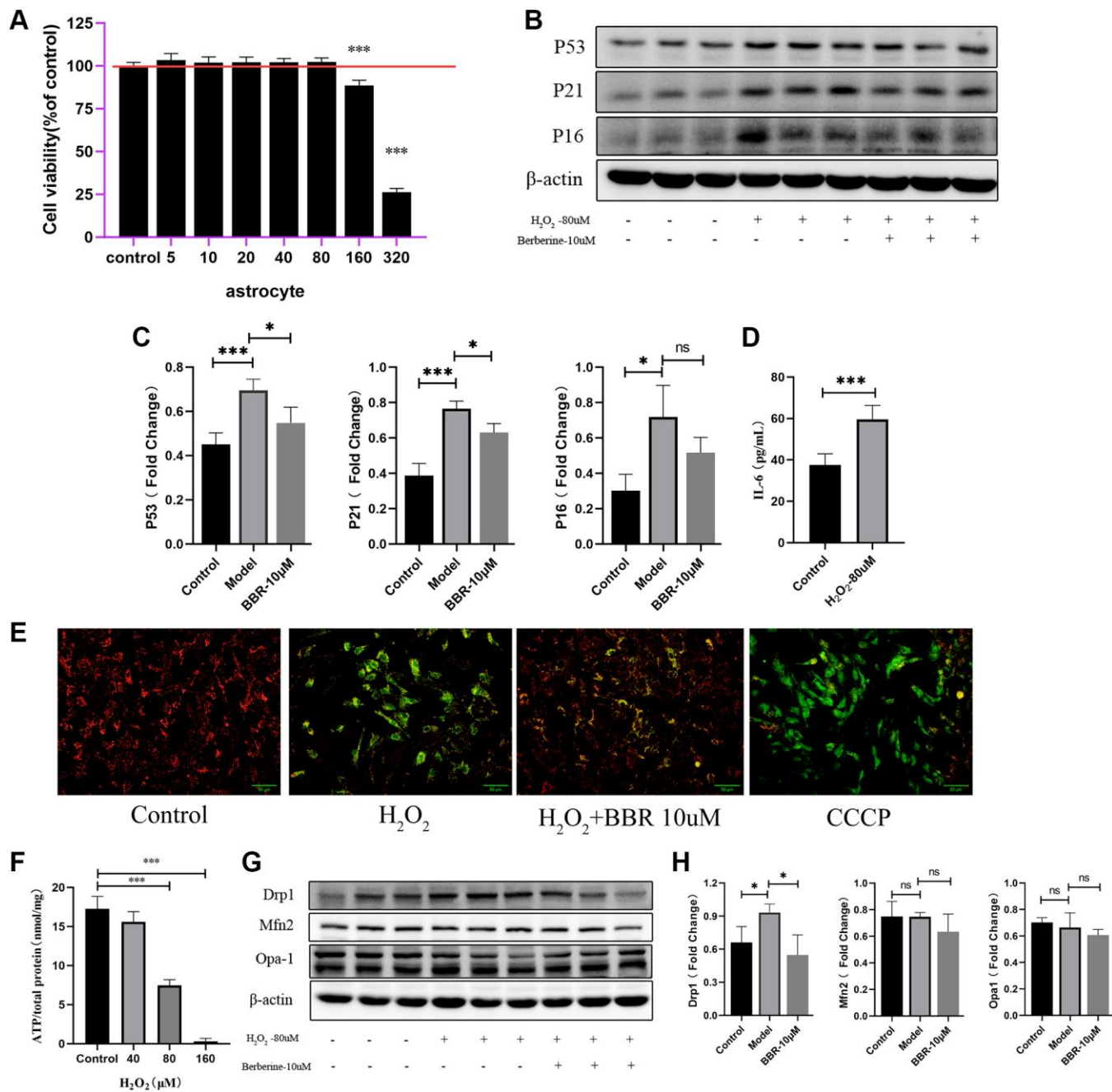


**Figure 4. Mitochondrial functions in aged astrocytes were found declined and berberine may have relieved effect.** (A) Cell viability assay of astrocytes by using different concentration of H<sub>2</sub>O<sub>2</sub>. (B) Representative immunoblots and (C) Quantitation of P53, P21, P16 and β-actin, in astrocytes treated with H<sub>2</sub>O<sub>2</sub> and berberine. β-actin was a loading control and data are expressed relative to control, *n* = 3. (D) Cytokine ELISA of IL-6 in culture medium of astrocytes treated with or without H<sub>2</sub>O<sub>2</sub>. (E) JC-1 staining. The red and green fluorescence reflects changes in the mitochondrial membrane potential of astrocytes treated with or without H<sub>2</sub>O<sub>2</sub> and berberine, the group of CCCP is used as a positive control. *n* = 3. ×200 magnification. (F) ATP content was detected by the ATP Assess Kit. (G) Representative immunoblots and (H) Quantitation of Drp1, Mfn2, Opa-1 and β-actin, in astrocytes treated with H<sub>2</sub>O<sub>2</sub> and berberine. β-actin was a loading control and data are expressed relative to control, *n* = 3. All experiments were expressed as the mean ±S.D, analyzed by ANOVA followed by Tukey's test, \**P* < 0.05, \*\**P* < 0.01, \*\*\**P* < 0.001, ns represents no significance.

neurodegenerative diseases. However, knowledge of the impact of senescent astrocytes in the brain is fragmented, and what's more troubling us is that it remains unclear how these senescent astrocytes may interact with microglia or neurons or any other cell types in the mammalian brain. In our *in vivo* aging model of mice, it has been found that the cognitive

decline was observed at 26 months. And mice in the 26-month-old group required more time to learn how to reach the platform than those in the 4-month-old group. The hippocampus is a content-addressable and autoassociative memory system wherein visual inputs from associational areas of the neocortex are processed through the CA1, CA2, CA3 and DG to the deep layers

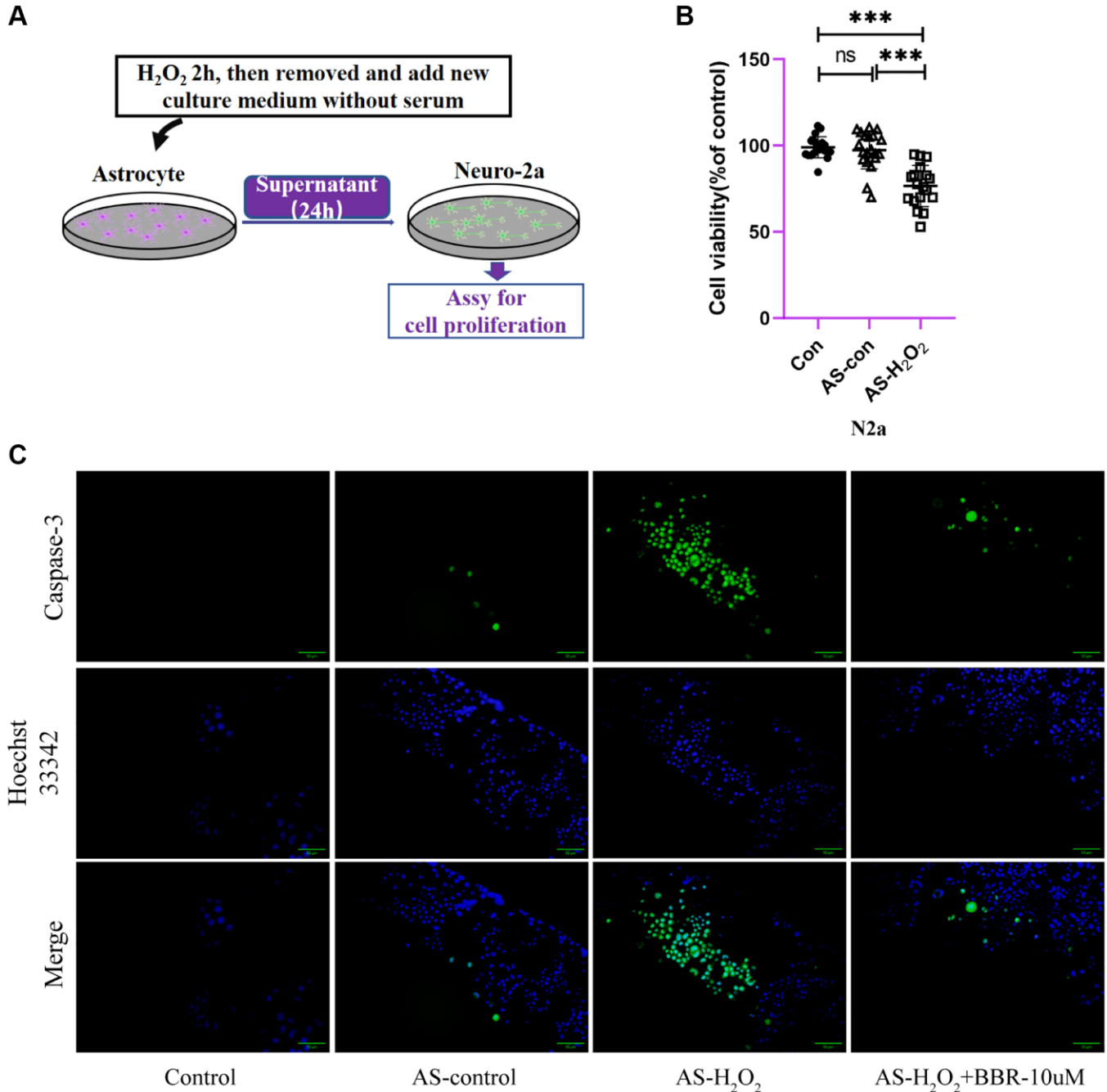


**Figure 5. The direct effect of aged astrocytes in communicating with neurons.** (A) A schematic diagram of the interaction of cell supernatants. (B) Cell viability assay of Neuro-2a cells by using astrocytes treated with or without H<sub>2</sub>O<sub>2</sub> supernatant. (C) Caspase-3 activity in Neuro-2a cells (treated with astrocytes-CM for 24 h). Green fluorescence indicates the activity of caspase-3. Blue indicates nuclear stained by Hoechst33342. Merge is the overlapped green and blue. ×200 magnification. All experiments were expressed as the mean ±S.D, analyzed by ANOVA followed by Tukey's test, \**P* < 0.05, \*\**P* < 0.01, \*\*\**P* < 0.001, ns represents no significance.



of the entorhinal cortex. Thus, HE staining was chosen to observe the morphological changes of the hippocampus in each group. The hippocampus of old mice showed thinning and loosening of pyramidal cells, as well as pyknotic and atrophied neurons, while the relative neuron loss of young mice was less than that of old mice, while the activation of microglia is more severe than those in young mice, which consistent with findings in other studies [15, 16]. However, finding interests us most is that through the co-immunostain of  $\beta$ -gal/P16<sup>INK4a</sup> and astrocytes marker GFAP, it could be found that this cell senescence marker appears in the

same position of astrocytes, meanwhile, transmission electron microphotographs showing that the mitochondria in aged mice may undergo malfunctioning, which suggests that astrocytes senescence may have occurred in the process of brain aging due to the mitochondrial dysfunction. Researchers have found that dysfunction of astrocytic mitochondria can cause deleterious actions on neurons [17, 18] and may bring adverse factors to other type of cells in brain [19]. Therefore, we made attempts to establish astrocytes models of aging *in vitro* to provide assistance in the study of brain aging.

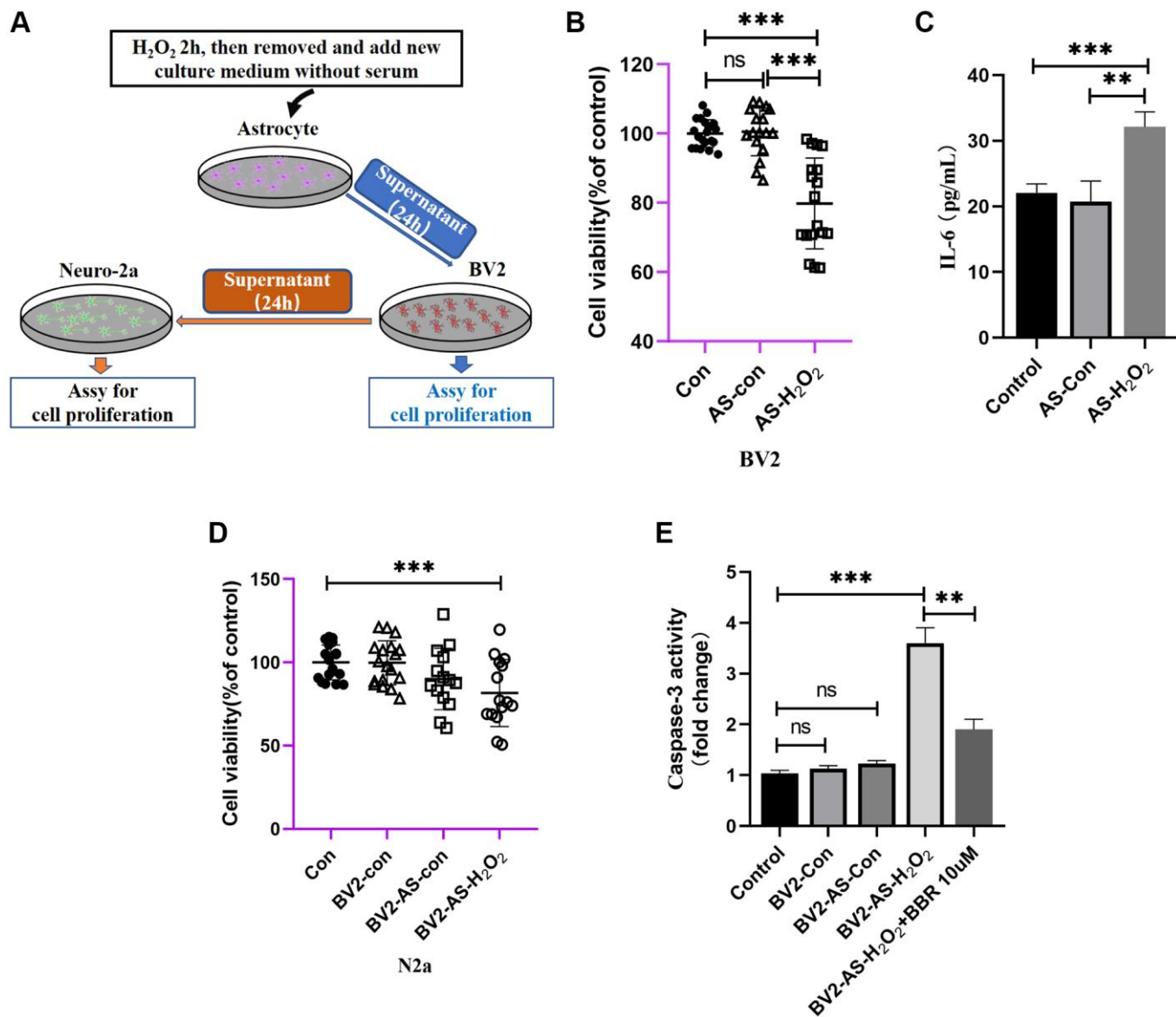


**Figure 6. The indirect effect of aged astrocytes in communicating with microglia and neurons.** (A) A schematic diagram of the interaction of cell supernatants. (B) Cell viability assay of BV2 cells by using astrocytes treated with or without H<sub>2</sub>O<sub>2</sub> supernatant. (C) Cytokine ELISA of IL-6 in culture medium of BV2 treated with astrocyte supernatant (treated with or without H<sub>2</sub>O<sub>2</sub>) expressed as pg cytokine per mL of culture medium without serum. (D) Cell viability assay of N2a cells by using BV2 treated with astrocytes supernatant. (E) The caspase-3 activity was measured with a caspase-3 assay kit. All experiments were expressed as the mean  $\pm$  S.D, analyzed by ANOVA followed by Tukey's test, \* $P < 0.05$ , \*\* $P < 0.01$ , \*\*\* $P < 0.001$ , ns represents no significance.

Several reports have shown that late passage of primary or mesenchymal stem cells can appear sign of senescence. The cultured primary MEF cells aged through later passage, which causes the cells to swell and eventually stop proliferating [20, 21]. The replicative senescence of astrocytes has also been confirmed in primary cultures derived from normal or post-AD brain tissue [22, 23]. During our experiments on astrocytes and adipocyte-derived mesenchymal stem cells, it was found that higher passage number cells have indeed reduced proliferative and differentiation capabilities (data not shown). Therefore, we here constructed a replicated aging model and oxidative stress model of astrocytes to imitate senescent cells during aging. Actually, previous articles have reported astrocytes that underwent serial passage cultivation or oxidative stress showed aged phenotypes like nuclear enlargement of primary astrocytes [24], elevated expression of P53 and P21 and P16 [25]. Senescence-associated beta-galactosidase, which is overexpressed and accumulated in the lysosomal specifically in senescent cells [26], and overexpressed P16<sup>INK4a</sup>, were widely used as cellular senescence markers. *In vitro* models in our study also found these similar changes of indicators. What's more is that the mitochondrial function of senescent astrocytes may decline with increased passaging [27], especially the level of proton leak and ATP, but we found that increased passaging did not affect the level of ATP (Supplementary Figure 1), which is different from the research before, speculating that this discrepancy may be caused by the difference of length of culturing time and self-regulation of astrocytes itself, but ATP level of the model of oxidative stress of astrocytes indeed changed. We also examined the mitochondrial membrane potential (MMP) and molecular changes in senescent astrocytes, found that no matter the serial passing model or the oxidative model of senescent astrocytes model all appeared MMP decline, which suggests that mitochondrial function is negatively affected. However, indeed, a drop in mitochondrial membrane potential does not necessarily lead to the loss of mitochondrial functions, research has reported that in Huntington's disease occurred imbalanced mitochondrial fusion-fission [28], our results showed that oxidative stress induced astrocytes senescence occurred with elevated expression of DRP1, suggests that fission in mitochondria of this type of senescent astrocytes were enhanced. Administration of berberine could ameliorate these mitochondrial dysfunctions caused by H<sub>2</sub>O<sub>2</sub> (the safe dosage of berberine administration was provided in Supplementary Figure 2). Thus, here leaves the question of how the mitochondrial dysfunction of senescent astrocytes does impact on the process of brain aging.

It has been proposed that astrocytes can establish communications with microglia, neurons and other astrocytes [29], and may involve in synapse formation

and elimination to different degrees in a wide range of disease conditions [30]. Astrocytes-microglia are considered to have immune-related functions in the mammalian brain. Initially, all the inflammatory responses or regulatory process are activated with the disruption of steady-state brain homeostasis. This rapid response induces the process of brain repair mostly by those activated glia cells. However, sustained secretion of inflammatory mediators of astrocytes or microglia may induce chronic inflammation, which usually happens in brain aging and finally may contribute to neurodegeneration and cognitive decline [31, 32]. Recently, research has found that a subset of microglia named as disease-associated microglia, which are associated with the genes of many of which were found in human genome that are linked to Alzheimer's disease (AD) and other neurodegenerative conditions [33–35]. This type of microglia will sustain secrete IL-6 and impact on neurons and finally lead to neuroinflammation. However, how the microglia be activated, numerous explanations are aroused. Some research suggests that microglial may be activated by a repertoire of pattern recognition receptors (PRRs) which allow microglia to detect “harmful signals” such as substances containing pathogen-associated molecular patterns (PAMPs) and damage-associated molecular patterns (DAMPs) including ATP or DNA or different types of interleukins released from astrocytes or other cell type in brain [36, 37]. Once upon detecting these messages, microglia migrate to those damaged positions and engulf those materials with an amoeboid-like “reactive” morphology [38, 39]. Our study found that in the brain of aged mice, the microglial morphology was significantly altered, and *in vitro* data also found that serial passaging or oxidative stress induced senescent astrocytes secreted higher IL-6 compared to those young-astrocytes, so these mitochondrial dysfunction or interleukin release by astrocytes may be a cause of microglia activation and finally lead to neurons death due to the sustained secrete of neuroinflammatory cytokines. Our cell viability assay of astrocytes-microglia-neuron also proved this cell-to-cell interaction would eventually lead to neuronal death.

Except for the astrocytes-microglia-neuron interaction referred above, our data also suggests that different types of senescent astrocytes could do damage to neurons directly. Although astrocytes were initially considered as nonfunctional fillers of the neuronal network. However, with time and technology advances, the significance of these types of cells for many complicated biological processes has been elucidated. *In vivo*, they interact closer with neurons and participate in the “tri-partite synapse”, which couples neurotransmission between pre- and postsynaptic materials [40]. Further contributions against trauma,

infection, and neurodegeneration to maintain neuronal health. However, many researches have reported that astrocytes senescence may directly influence neuronal health through multiple processes. Like SASP, P16, P21 [25, 41], which were referred to above, and DNA damage induced by ionizing radiation [42]. What's more, research also reported that ROS-induced senescence in human astrocytes showed downregulated genes of neuronal development and differentiation and upregulated genes of proinflammation [43], these may be partially responsible for the neuronal damage or death. In our study, we found that after neurons incubated with the supernatant of senescent astrocytes, the viability was dramatically decreased, combined with elevated caspase-3 expression compared to those astrocytes treated without H<sub>2</sub>O<sub>2</sub>. Interestingly, these adverse effects were ameliorated upon inclusion of berberine when inducing oxidative stress with H<sub>2</sub>O<sub>2</sub>. These results suggest that senescent astrocytes could do impact on neuronal survive in a direct way.

Meanwhile, we used berberine as a positive control to deal with the dysfunction of mitochondria induced by oxidative stress, since it had long been reported to have the function of mitochondria targeting and previous studies also proved that it could possess several pharmacological properties [44–47], including anti-inflammatory, antifibrotic, and correct the fission of mitochondria. Our data show that berberine may have the favorable potency of astrocytes from escaping the process of senescence.

## CONCLUSIONS

In summary, we have shown that *in vivo*, astrocytes may be the earliest sign of aging in numerous types of brain cells, and senescent astrocytes could trigger neurons' death both direct and indirect ways. However, future investigation on cell-to-cell interactions and the decent mechanism of them are needed. Astrocytes senescence is a brand-new field of study and more research needs to be designed and implemented so that the autonomous and non-autonomous mechanisms of senescent astrocytes and its bandage between age-related neurodegenerative diseases would eventually be uncovered.

## AUTHOR CONTRIBUTIONS

WZ and XY designed the overall research experiments. MZ and LC performed the experiments. WZ and JL analyzed the data. WZ, XY wrote and revised the manuscript.

## CONFLICTS OF INTEREST

The authors declare no conflicts of interest related to this study.

## ETHICAL STATEMENT

Animal welfare and experimental procedures complied with the Provisions and General Recommendations of the Chinese Experimental Animals Administration Legislation. All animal experimental procedures were approved by the Ethics Committee for the Use of Experimental Animals of College of Basic medical Sciences, Jilin University [SCXK (Jing) 2014-0004]. All efforts were carried out to reduce the number of animals used and minimize animal suffering.

## FUNDING

This research was funded by Preclinical Pharmacology R&D Center of Jilin Province (No. 20170623062TC), Science and technology development projects of Jilin Province (No. 20190304029YY; No. 20190201144JC).

## REFERENCES

1. Baker DJ, Childs BG, Durik M, Wijers ME, Sieben CJ, Zhong J, Saltness RA, Jeganathan KB, Verzosa GC, Pezeshki A, Khazaie K, Miller JD, van Deursen JM. Naturally occurring p16(Ink4a)-positive cells shorten healthy lifespan. *Nature*. 2016; 530:184–9. <https://doi.org/10.1038/nature16932> PMID:[26840489](https://pubmed.ncbi.nlm.nih.gov/26840489/)
2. Tabula Muris Consortium. A single-cell transcriptomic atlas characterizes ageing tissues in the mouse. *Nature*. 2020; 583:590–5. <https://doi.org/10.1038/s41586-020-2496-1> PMID:[32669714](https://pubmed.ncbi.nlm.nih.gov/32669714/)
3. Schaum N, Lehallier B, Hahn O, Pálovics R, Hosseinzadeh S, Lee SE, Sit R, Lee DP, Losada PM, Zardeneta ME, Fehlmann T, Webber JT, McGeever A, et al, and Tabula Muris Consortium. Ageing hallmarks exhibit organ-specific temporal signatures. *Nature*. 2020; 583:596–602. <https://doi.org/10.1038/s41586-020-2499-y> PMID:[32669715](https://pubmed.ncbi.nlm.nih.gov/32669715/)
4. Hill SA, Blaeser AS, Coley AA, Xie Y, Shepard KA, Harwell CC, Gao WJ, Garcia ADR. Sonic hedgehog signaling in astrocytes mediates cell type-specific synaptic organization. *Elife*. 2019; 8:e45545. <https://doi.org/10.7554/elife.45545> PMID:[31194676](https://pubmed.ncbi.nlm.nih.gov/31194676/)
5. Valori CF, Guidotti G, Brambilla L, Rossi D. Astrocytes: Emerging Therapeutic Targets in Neurological Disorders. *Trends Mol Med*. 2019; 25:750–9. <https://doi.org/10.1016/j.molmed.2019.04.010> PMID:[31122805](https://pubmed.ncbi.nlm.nih.gov/31122805/)



6. Romanos J, Thieren L, Santello M. Diving into new depths of astrocyte signaling. *Nat Neurosci.* 2019; 22:1749–50.  
<https://doi.org/10.1038/s41593-019-0513-1>  
PMID:[31570864](https://pubmed.ncbi.nlm.nih.gov/31570864/)
7. Zou W, Song Y, Li Y, Du Y, Zhang X, Fu J. The Role of Autophagy in the Correlation Between Neuron Damage and Cognitive Impairment in Rat Chronic Cerebral Hypoperfusion. *Mol Neurobiol.* 2018; 55:776–91.  
<https://doi.org/10.1007/s12035-016-0351-z>  
PMID:[28058581](https://pubmed.ncbi.nlm.nih.gov/28058581/)
8. Dos-Santos-Pereira M, Acuña L, Hamadat S, Rocca J, González-Lizárraga F, Chehín R, Sepulveda-Díaz J, Del-Bel E, Raisman-Vozari R, Michel PP. Microglial glutamate release evoked by  $\alpha$ -synuclein aggregates is prevented by dopamine. *Glia.* 2018; 66:2353–65.  
<https://doi.org/10.1002/glia.23472>  
PMID:[30394585](https://pubmed.ncbi.nlm.nih.gov/30394585/)
9. Streit WJ, Walter SA, Pennell NA. Reactive microgliosis. *Prog Neurobiol.* 1999; 57:563–81.  
[https://doi.org/10.1016/s0301-0082\(98\)00069-0](https://doi.org/10.1016/s0301-0082(98)00069-0)  
PMID:[10221782](https://pubmed.ncbi.nlm.nih.gov/10221782/)
10. Ritschka B, Storer M, Mas A, Heinzmann F, Ortells MC, Morton JP, Sansom OJ, Zender L, Keyes WM. The senescence-associated secretory phenotype induces cellular plasticity and tissue regeneration. *Genes Dev.* 2017; 31:172–83.  
<https://doi.org/10.1101/gad.290635.116>  
PMID:[28143833](https://pubmed.ncbi.nlm.nih.gov/28143833/)
11. Kodali M, Attaluri S, Madhu LN, Shuai B, Upadhy R, Gonzalez JJ, Rao X, Shetty AK. Metformin treatment in late middle age improves cognitive function with alleviation of microglial activation and enhancement of autophagy in the hippocampus. *Aging Cell.* 2021; 20:e13277.  
<https://doi.org/10.1111/accel.13277>  
PMID:[33443781](https://pubmed.ncbi.nlm.nih.gov/33443781/)
12. Chun H, Im H, Kang YJ, Kim Y, Shin JH, Won W, Lim J, Ju Y, Park YM, Kim S, Lee SE, Lee J, Woo J, et al. Severe reactive astrocytes precipitate pathological hallmarks of Alzheimer's disease via  $H_2O_2$  production. *Nat Neurosci.* 2020; 23:1555–66.  
<https://doi.org/10.1038/s41593-020-00735-y>  
PMID:[33199896](https://pubmed.ncbi.nlm.nih.gov/33199896/)
13. Sompol P, Furman JL, Pleiss MM, Kraner SD, Artiushin IA, Batten SR, Quintero JE, Simmerman LA, Beckett TL, Lovell MA, Murphy MP, Gerhardt GA, Norris CM. Calcineurin/NFAT Signaling in Activated Astrocytes Drives Network Hyperexcitability in  $A\beta$ -Bearing Mice. *J Neurosci.* 2017; 37:6132–48.  
<https://doi.org/10.1523/JNEUROSCI.0877-17.2017>  
PMID:[28559377](https://pubmed.ncbi.nlm.nih.gov/28559377/)
14. Fiebig C, Keiner S, Ebert B, Schäffner I, Jagasia R, Lie DC, Beckervordersandforth R. Mitochondrial Dysfunction in Astrocytes Impairs the Generation of Reactive Astrocytes and Enhances Neuronal Cell Death in the Cortex Upon Photothrombotic Lesion. *Front Mol Neurosci.* 2019; 12:40.  
<https://doi.org/10.3389/fnmol.2019.00040>  
PMID:[30853890](https://pubmed.ncbi.nlm.nih.gov/30853890/)
15. Kwon HS, Koh SH. Neuroinflammation in neurodegenerative disorders: the roles of microglia and astrocytes. *Transl Neurodegener.* 2020; 9:42.  
<https://doi.org/10.1186/s40035-020-00221-2>  
PMID:[33239064](https://pubmed.ncbi.nlm.nih.gov/33239064/)
16. Yang H, Wang H, Ren J, Chen Q, Chen ZJ. cGAS is essential for cellular senescence. *Proc Natl Acad Sci U S A.* 2017; 114:E4612–20.  
<https://doi.org/10.1073/pnas.1705499114>  
PMID:[28533362](https://pubmed.ncbi.nlm.nih.gov/28533362/)
17. Glück S, Guey B, Gulen MF, Wolter K, Kang TW, Schmacke NA, Bridgeman A, Rehwinkel J, Zender L, Ablasser A. Innate immune sensing of cytosolic chromatin fragments through cGAS promotes senescence. *Nat Cell Biol.* 2017; 19:1061–70.  
<https://doi.org/10.1038/ncb3586>  
PMID:[28759028](https://pubmed.ncbi.nlm.nih.gov/28759028/)
18. Evans RJ, Wyllie FS, Wynford-Thomas D, Kipling D, Jones CJ. A P53-dependent, telomere-independent proliferative life span barrier in human astrocytes consistent with the molecular genetics of glioma development. *Cancer Res.* 2003; 63:4854–61.  
PMID:[12941806](https://pubmed.ncbi.nlm.nih.gov/12941806/)
19. Blasko I, Stampfer-Kountchev M, Robatscher P, Veerhuis R, Eikelenboom P, Grubeck-Loebenstien B. How chronic inflammation can affect the brain and support the development of Alzheimer's disease in old age: the role of microglia and astrocytes. *Aging Cell.* 2004; 3:169–76.  
<https://doi.org/10.1111/j.1474-9728.2004.00101.x>  
PMID:[15268750](https://pubmed.ncbi.nlm.nih.gov/15268750/)
20. Yoon KB, Park KR, Kim SY, Han SY. Induction of Nuclear Enlargement and Senescence by Sirtuin Inhibitors in Glioblastoma Cells. *Immune Netw.* 2016; 16:183–8.  
<https://doi.org/10.4110/in.2016.16.3.183>  
PMID:[27340387](https://pubmed.ncbi.nlm.nih.gov/27340387/)
21. Bitto A, Sell C, Crowe E, Lorenzini A, Malaguti M, Hrelia S, Torres C. Stress-induced senescence in human and rodent astrocytes. *Exp Cell Res.* 2010; 316:2961–8.  
<https://doi.org/10.1016/j.yexcr.2010.06.021>  
PMID:[20620137](https://pubmed.ncbi.nlm.nih.gov/20620137/)
22. Lee BY, Han JA, Im JS, Morrone A, Johung K, Goodwin EC, Kleijer WJ, DiMaio D, Hwang ES. Senescence-

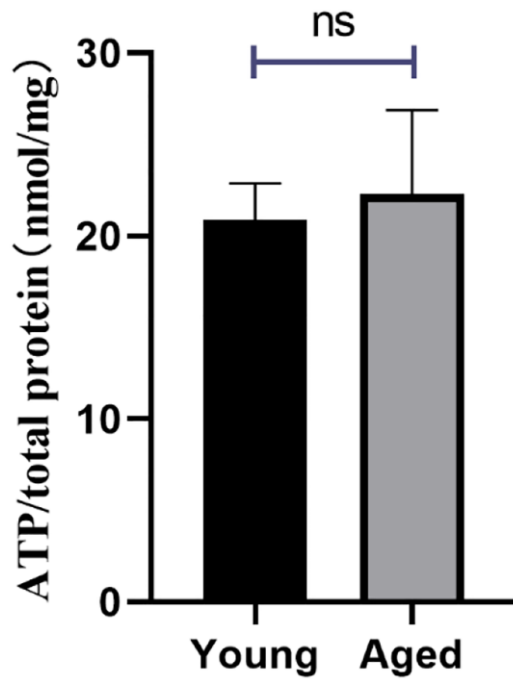
- associated beta-galactosidase is lysosomal beta-galactosidase. *Aging Cell*. 2006; 5:187–95.  
<https://doi.org/10.1111/j.1474-9726.2006.00199.x>  
PMID:[16626397](https://pubmed.ncbi.nlm.nih.gov/16626397/)
23. Bang M, Gonzales EL, Shin CY, Kwon KJ. Late Passage Cultivation Induces Aged Astrocyte Phenotypes in Rat Primary Cultured Cells. *Biomol Ther (Seoul)*. 2021; 29:144–53.  
<https://doi.org/10.4062/biomolther.2020.175>  
PMID:[33262320](https://pubmed.ncbi.nlm.nih.gov/33262320/)
  24. Oliver D, Reddy PH. Dynamics of Dynamin-Related Protein 1 in Alzheimer's Disease and Other Neurodegenerative Diseases. *Cells*. 2019; 8:961.  
<https://doi.org/10.3390/cells8090961>  
PMID:[31450774](https://pubmed.ncbi.nlm.nih.gov/31450774/)
  25. Griffin WS, Sheng JG, Royston MC, Gentleman SM, McKenzie JE, Graham DI, Roberts GW, Mrak RE. Glial-neuronal interactions in Alzheimer's disease: the potential role of a 'cytokine cycle' in disease progression. *Brain Pathol*. 1998; 8:65–72.  
<https://doi.org/10.1111/j.1750-3639.1998.tb00136.x>  
PMID:[9458167](https://pubmed.ncbi.nlm.nih.gov/9458167/)
  26. Gollihue JL, Norris CM. Astrocyte mitochondria: Central players and potential therapeutic targets for neurodegenerative diseases and injury. *Ageing Res Rev*. 2020; 59:101039.  
<https://doi.org/10.1016/j.arr.2020.101039>  
PMID:[32105849](https://pubmed.ncbi.nlm.nih.gov/32105849/)
  27. Mendiola AS, Ryu JK, Bardehle S, Meyer-Franke A, Ang KK, Wilson C, Baeten KM, Hanspers K, Merlini M, Thomas S, Petersen MA, Williams A, Thomas R, et al. Transcriptional profiling and therapeutic targeting of oxidative stress in neuroinflammation. *Nat Immunol*. 2020; 21:513–24.  
<https://doi.org/10.1038/s41590-020-0654-0>  
PMID:[32284594](https://pubmed.ncbi.nlm.nih.gov/32284594/)
  28. Morales I, Guzmán-Martínez L, Cerda-Troncoso C, Farías GA, Maccioni RB. Neuroinflammation in the pathogenesis of Alzheimer's disease. A rational framework for the search of novel therapeutic approaches. *Front Cell Neurosci*. 2014; 8:112.  
<https://doi.org/10.3389/fncel.2014.00112>  
PMID:[24795567](https://pubmed.ncbi.nlm.nih.gov/24795567/)
  29. Keren-Shaul H, Spinrad A, Weiner A, Matcovitch-Natan O, Dvir-Szternfeld R, Ulland TK, David E, Baruch K, Lara-Astaiso D, Toth B, Itzkovitz S, Colonna M, Schwartz M, Amit I. A Unique Microglia Type Associated with Restricting Development of Alzheimer's Disease. *Cell*. 2017; 169:1276–90.e17.  
<https://doi.org/10.1016/j.cell.2017.05.018>  
PMID:[28602351](https://pubmed.ncbi.nlm.nih.gov/28602351/)
  30. Lambert JC, Grenier-Boley B, Harold D, Zelenika D, Chouraki V, Kamatani Y, Sleegers K, Ikram MA, Hiltunen M, Reitz C, Mateo I, Feulner T, Bullido M, et al. Genome-wide haplotype association study identifies the FRMD4A gene as a risk locus for Alzheimer's disease. *Mol Psychiatry*. 2013; 18:461–70.  
<https://doi.org/10.1038/mp.2012.14>  
PMID:[22430674](https://pubmed.ncbi.nlm.nih.gov/22430674/)
  31. Yeh CW, Liu HK, Lin LC, Liou KT, Huang YC, Lin CH, Tzeng TT, Shie FS, Tsay HJ, Shiao YJ. Xuefu Zhuyu decoction ameliorates obesity, hepatic steatosis, neuroinflammation, amyloid deposition and cognition impairment in metabolically stressed APPswe/PS1dE9 mice. *J Ethnopharmacol*. 2017; 209:50–61.  
<https://doi.org/10.1016/j.jep.2017.07.036>  
PMID:[28743670](https://pubmed.ncbi.nlm.nih.gov/28743670/)
  32. Hirsiger S, Simmen HP, Werner CM, Wanner GA, Rittirsch D. Danger signals activating the immune response after trauma. *Mediators Inflamm*. 2012; 2012:315941.  
<https://doi.org/10.1155/2012/315941>  
PMID:[22778496](https://pubmed.ncbi.nlm.nih.gov/22778496/)
  33. Kigerl KA, de Rivero Vaccari JP, Dietrich WD, Popovich PG, Keane RW. Pattern recognition receptors and central nervous system repair. *Exp Neurol*. 2014; 258:5–16.  
<https://doi.org/10.1016/j.expneurol.2014.01.001>  
PMID:[25017883](https://pubmed.ncbi.nlm.nih.gov/25017883/)
  34. Torres-Platas SG, Comeau S, Rachalski A, Bo GD, Cruceanu C, Turecki G, Giros B, Mechawar N. Morphometric characterization of microglial phenotypes in human cerebral cortex. *J Neuroinflammation*. 2014; 11:12.  
<https://doi.org/10.1186/1742-2094-11-12>  
PMID:[24447857](https://pubmed.ncbi.nlm.nih.gov/24447857/)
  35. Kumar A, Stoica BA, Sabirzhanov B, Burns MP, Faden AI, Loane DJ. Traumatic brain injury in aged animals increases lesion size and chronically alters microglial/macrophage classical and alternative activation states. *Neurobiol Aging*. 2013; 34:1397–411.  
<https://doi.org/10.1016/j.neurobiolaging.2012.11.013>  
PMID:[23273602](https://pubmed.ncbi.nlm.nih.gov/23273602/)
  36. Araque A, Parpura V, Sanzgiri RP, Haydon PG. Tripartite synapses: glia, the unacknowledged partner. *Trends Neurosci*. 1999; 22:208–15.  
[https://doi.org/10.1016/s0166-2236\(98\)01349-6](https://doi.org/10.1016/s0166-2236(98)01349-6)  
PMID:[10322493](https://pubmed.ncbi.nlm.nih.gov/10322493/)
  37. Bhat R, Crowe EP, Bitto A, Moh M, Katsetos CD, Garcia FU, Johnson FB, Trojanowski JQ, Sell C, Torres C. Astrocyte senescence as a component of Alzheimer's disease. *PLoS One*. 2012; 7:e45069.  
<https://doi.org/10.1371/journal.pone.0045069>  
PMID:[22984612](https://pubmed.ncbi.nlm.nih.gov/22984612/)
  38. Zou Y, Zhang N, Ellerby LM, Davalos AR, Zeng X, Campisi J, Desprez PY. Responses of human

- embryonic stem cells and their differentiated progeny to ionizing radiation. *Biochem Biophys Res Commun.* 2012; 426:100–5.  
<https://doi.org/10.1016/j.bbrc.2012.08.043>  
PMID:22917535
39. Crowe EP, Tuzer F, Gregory BD, Donahue G, Gosai SJ, Cohen J, Leung YY, Yetkin E, Nativio R, Wang LS, Sell C, Bonini NM, Berger SL, et al. Changes in the Transcriptome of Human Astrocytes Accompanying Oxidative Stress-Induced Senescence. *Front Aging Neurosci.* 2016; 8:208.  
<https://doi.org/10.3389/fnagi.2016.00208>  
PMID:27630559
40. Chen YY, Li RY, Shi MJ, Zhao YX, Yan Y, Xu XX, Zhang M, Zhao XT, Zhang YB. Demethyleneberberine alleviates inflammatory bowel disease in mice through regulating NF- $\kappa$ B signaling and T-helper cell homeostasis. *Inflamm Res.* 2017; 66:187–96.  
<https://doi.org/10.1007/s00011-016-1005-3>  
PMID:27900412
41. Qiang X, Xu L, Zhang M, Zhang P, Wang Y, Wang Y, Zhao Z, Chen H, Liu X, Zhang Y. Demethyleneberberine attenuates non-alcoholic fatty liver disease with activation of AMPK and inhibition of oxidative stress. *Biochem Biophys Res Commun.* 2016; 472:603–9.  
<https://doi.org/10.1016/j.bbrc.2016.03.019>  
PMID:26970305
42. Zhang P, Qiang X, Zhang M, Ma D, Zhao Z, Zhou C, Liu X, Li R, Chen H, Zhang Y. Demethyleneberberine, a natural mitochondria-targeted antioxidant, inhibits mitochondrial dysfunction, oxidative stress, and steatosis in alcoholic liver disease mouse model. *J Pharmacol Exp Ther.* 2015; 352:139–47.  
<https://doi.org/10.1124/jpet.114.219832>  
PMID:25362106
43. Lin C, Yang X, Li H, Zou Y, Mohammad IS, Rong H, Rao Y, Song J, Leung SSY, Hu H. Self-assembled nanomedicine combining a berberine derivative and doxorubicin for enhanced antitumor and antimetastatic efficacy via mitochondrial pathways. *Nanoscale.* 2021; 13:6605–23.  
<https://doi.org/10.1039/d1nr00032b>  
PMID:33885540
44. Hayakawa K, Esposito E, Wang X, Terasaki Y, Liu Y, Xing C, Ji X, Lo EH. Transfer of mitochondria from astrocytes to neurons after stroke. *Nature.* 2016; 535:551–5.  
<https://doi.org/10.1038/nature18928>  
PMID:27466127
45. Chen QM, Bartholomew JC, Campisi J, Acosta M, Reagan JD, Ames BN. Molecular analysis of H2O2-induced senescent-like growth arrest in normal human fibroblasts: p53 and Rb control G1 arrest but not cell replication. *Biochem J.* 1998; 332:43–50.  
<https://doi.org/10.1042/bj3320043>  
PMID:9576849
46. Griscelli F, Li H, Cheong C, Opolon P, Bennaceur-Griscelli A, Vassal G, Soria J, Soria C, Lu H, Perricaudet M, Yeh P. Combined effects of radiotherapy and angiostatin gene therapy in glioma tumor model. *Proc Natl Acad Sci U S A.* 2000; 97:6698–703.  
<https://doi.org/10.1073/pnas.110134297>  
PMID:10823901
47. Camandola S, Mattson MP. Brain metabolism in health, aging, and neurodegeneration. *EMBO J.* 2017; 36:1474–92.  
<https://doi.org/10.15252/embi.201695810>  
PMID:28438892

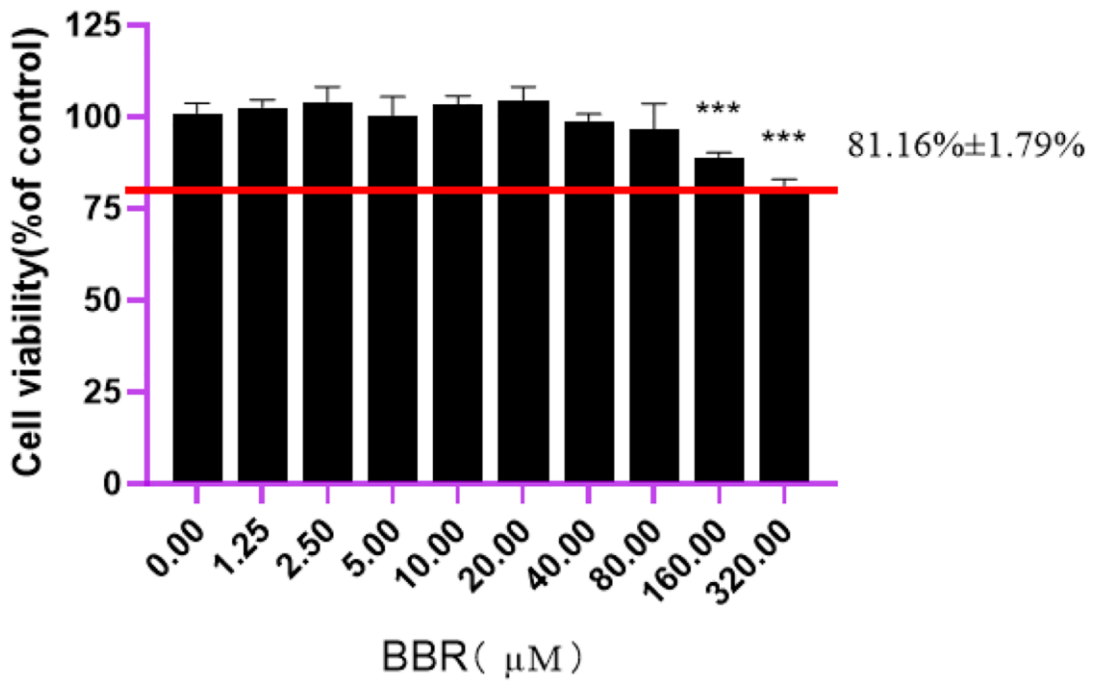


SUPPLEMENTARY MATERIALS

Supplementary Figures



Supplementary Figure 1. The intracellular ATP level of young and aged astrocytes.



Supplementary Figure 2. The viability of astrocytes treated with different concentration of berberine